Journal of Pharmaceutical Analysis 11 (2021) 646–652

Contents lists available at ScienceDirect

Journal of Pharmaceutical Analysis

journal homepage: www.elsevier.com/locate/jpa

Original article

A sensitive electrochemical detection of metronidazole in synthetic serum and urine samples using low-cost screen-printed electrodes modified with reduced graphene oxide and C60

Elsa Maria Materón [a, b], Ademar Wong [a, *], Tayane Aguiar Freitas [a], Ronaldo Censi Faria [a], Osvaldo N. Oliveira Jr. [b]

[a] Department of Chemistry, Federal University of São Carlos, 13560-970, São Carlos, Brazil
[b] São Carlos Institute of Physics, University of São Paulo, 13560-970, São Carlos, Brazil

ARTICLE INFO

Article history:
Received 15 June 2020
Received in revised form
30 January 2021
Accepted 18 March 2021
Available online 25 March 2021

Keywords:
Metronidazole
Fullerene
Reduced graphene oxide
Screen-printed electrodes
Antibiotic

ABSTRACT

Monitoring the concentration of antibiotics in body fluids is essential to optimizing the therapy and minimizing the risk of bacteria resistance, which can be made with electrochemical sensors tailored with appropriate materials. In this paper, we report on sensors made with screen-printed electrodes (SPE) coated with fullerene (C60), reduced graphene oxide (rGO) and Nafion (NF) (C60-rGO-NF/SPE) to determine the antibiotic metronidazole (MTZ). Under optimized conditions, the C60-rGO-NF/SPE sensor exhibited a linear response in square wave voltammetry for MTZ concentrations from 2.5×10^{-7} to 34×10^{-6} mol/L, with a detection limit of 2.1×10^{-7} mol/L. This sensor was also capable of detecting MTZ in serum and urine, with recovery between 94% and 100%, which are similar to those of the standard chromatographic method (HPLC-UV). Because the C60-rGO-NF/SPE sensor is amenable to mass production and allows for MTZ determination with simple principles of detection, it fulfills the requirements of therapeutic drug monitoring programs.

1. Introduction

The alarming increase in bacteria resistance has brought failure to many treatments requiring antibiotics [1], which is especially worrying because introducing new drugs into the market is expensive and takes a long time. New approaches are therefore needed to preserve the efficacy of currently approved antibiotics [2], as exemplified by the therapeutic drug monitoring (TDM) program used in clinical practice to quantify concentrations of antibiotics and other drugs in body fluids [2,3]. With TDM combined with knowledge from pharmacokinetics, one may identify situations where an unnecessary amount of drug has been administered, and optimize the concentration which would inhibit bacterial growth [4,5]. An important requirement for the success of TDM is to develop low-cost, easy-to-use tests to quantify the drugs in body fluids. Today, this type of test is performed with expensive, time-consuming methods, including radioimmunoassays, high-performance liquid chromatography (HPLC), fluorescence polarization immunoassay, enzyme immunoassay, and enzyme-linked immunosorbant assay [6–9]. In this context, electrochemical sensors and biosensors are strong candidates to fulfill the TDM requirements, for they have been proven excellent in the monitoring of antimicrobial drugs [10–12], in addition to the detection of antibiotics in water [10,13], food [14,15], and biological samples [16,17].

The development of efficient electrochemical sensors for TDM which are also of low cost, demands a judicious choice of materials, both for the electrodes and coating layers used in functionalization. From the large library of materials for this purpose, carbon nanomaterials (e.g., graphite, nanohorns, fullerenes, carbon nanotubes, graphene, carbon nanoparticles, and nanodiamonds) should be highlighted for their reproducible electrocatalytic responses, biocompatibility and enhanced electron transport [18,19]. In this study, we chose carbon ink to produce screen-printed electrode (SPE) amenable for mass production [20], which was modified by two other types of carbon nanomaterials, namely, reduced graphene oxide (rGO) and fullerene (C60) in order to leverage their intrinsic properties such as increased active area, suitability for

Peer review under responsibility of Xi'an Jiaotong University.
* Corresponding author.
E-mail address: ademar.wong@hotmail.com (A. Wong).

https://doi.org/10.1016/j.jpha.2021.03.004

immobilization of electrocatalytic compounds and easy fabrication [21]. Fullerenes have been widely used as nanomediator for sensors since they allow for operation at lower potentials, thus reducing the interference from electroactive compounds [22–27].

We tested the suitability of the electrochemical sensors by determining the concentration of metronidazole (MTZ), a synthetic antibiotic to treat trichomoniasis, dysentery, liver abscesses, rosacea and anaerobically infected burn wounds, in addition to surgical prophylaxis [28,29]. For patients with burn wounds, in particular, sepsis is a major cause of morbidity and mortality due to the inability to maintain a sterile environment in the hospital and avoid contamination with microorganisms and their ensuing antibiotic resistance [2,30,31]. Detection of MTZ is also relevant to minimizing its side effects, which include nauseas, diarrhea, neurotoxicity, optic neuropathy, peripheral neurophaty and ancephatopathy. Furthermore, it has shown genotoxic effects in animal models [28]. The electrochemical sensors reported to determine MTZ were made with molecularly imprinted polymers [32–36], β-cyclodextrin-functionalized gold nanoparticles/poly(L-cysteine) [37], 3D hierarchical porous graphene/polythionine [38], Ni/Fe-layered double hydroxides [39], modified glassy carbon electrodes, multiwalled carbon nanotubes [40], composite film derived from cysteic acid, poly(diallydimethylammonium chloride)-functionalized graphene [41], and carbon paste electrode [42–44] in pharmaceutical drug tablets and fish tissue [32,33,40], and human blood serum [35]. In this work, we employed C60-rGO and Nafion, for the first time to the best of our knowledge, to modify a low-cost SPE.

2. Materials and methods

2.1. Reagents, materials, and apparatus

MTZ, clindamycin, dipyrone, tetracycline, diclofenac, ranitidine, uric acid, caffeine and C60 were purchased from Sigma-Aldrich (São Paulo, Brazil). Graphene was obtained from Graphene Supermarket (Calverton, MD, USA). A stock solution of MTZ at 1.0×10^{-2} mol/L was prepared by diluting 17.1 mg in a 10 mL capacity flask. The electrochemical measurements were performed with an Autolab potentiostat/galvanostat (model PGSTAT-30, Eco Chemie, Utrecht, The Netherlands) controlled by NOVA 2.1 software. The electrochemical system had a screen-printed sensor with three-electrodes: pseudo-reference electrode (Ag/AgCl), auxiliary electrode made of carbon ink and the working electrode with functionalized carbon ink (r=0.15 cm) connected with an auxiliary cable.

HPLC-UV analysis was made with a Shimadzu model 10ATvp LC system (San Francisco, CA, USA), consisting of two pumps (LC-10AT), column oven (CTO10A), and UV detector (SPD-10A). The mobile phase consisted of a 1.0×10^{-3} mol/L phosphate buffer (pH 7.0) solution and acetonitrile at the ratio of 95:5 (*V/V*) (filtered through a 0.22 μm pore membrane filter) at the temperature of 20 °C. The flow rate was 1 mL/min and detection was made at 320 nm. This analytical method was used for the comparison with the electrochemical sensor [45].

2.2. Fabrication and preparation of C60-rGO-NF/SPE sensors

SPE were made as reported in the literature [46,47]. A negative mask with the SPE model was prepared in an adhesive vinyl polymeric material using Silhouette Studio version 2.7.4 software and an electronic craft cutter from Silhouette Cameo (Silhouette America, São Paulo, Brazil). Fig. 1 shows the main steps for preparing the electrode: (1) the vinyl mask was fixed on a polyester sheet (USA Folien Laserjet Clear A4 transparency film); (2) the carbon ink (C2160602D2 from Gwent Electronic Materials Ltd., São Paulo, Brazil) was deposited on the support with a plastic spatula and cured at 90 °C for 30 min; (3) the Ag/AgCl ink (C2051014P10, Gwent Electronic Materials Ltd., São Paulo, Brazil) was applied to the part corresponding to the pseudo-reference electrode, and then the ink was cured at 60 °C for 30 min; (4) removal of the vinyl mask; (5) delimitation of the geometric area of the working electrodes with a rectangular vinyl mask, followed by a heater press and (6) SPE for use.

To obtain an active sensor, the SPE was placed in an acid bath (0.5 mol/L H_2SO_4) under stirring for 1 min (for partial functionalization of the electrode surface). A suspension (2 mL) containing rGO (3 mg) and NF (50 μL, 0.5% *V/V*) was prepared and subjected to an ultrasonic bath for 20 min to yield a homogeneous dispersion. An aliquot of 3 μL of C60 solution prepared in CH_2Cl_2 was cast onto the electrode surface, and dried for 1 h. In the pretreatment process cyclic voltammetry (2 cycles) was used with the potential scanning from 0 to −1.5 V at a scan rate of 20 mV/s in a 1 mol/L KOH solution. Another potential scanning was carried out (550 to −50 mV) at a scan rate of 50 mV/s using the phosphate buffer solution (pH 7.0) with the goal of stabilizing the electrochemical sensor response [48].

2.3. Preparation of synthetic urine and serum samples

The synthetic urine sample was prepared by following the procedure reported by Laube et al. [49] using the compounds found in real samples: 49, 20, 10, 15, 18, 18 mmol/L of NaCl, KCl, $CaCl_2$, KH_2PO_4, NH_4Cl, and urea were added. The remaining volume of the flask was filled with ultrapure water. The synthetic serum sample was prepared as described by Parham and Zargar [50]. The flask volume was completed with ultrapure water. The total volume of the samples was 25 mL. After this step, the samples were spiked with two levels of concentration of MTZ and an aliquot of 250 μL was added separately in 10 mL of supporting electrolyte solution.

3. Results and discussion

3.1. Morphological characterization of the C60-rGO-NF/SPE sensor

The scanning electron microscopy image in Fig. 2A is typical of rGO, with smooth multilayers in overlapping sheets with crumpled and wrinkled sheets. Fig. 2B shows a dense, uniform C60 film deposited on rGO, resulting from an evenly dispersed C60-rGO mixture which had been subjected to an ultrasound bath before modifying the surface electrode. NF is very diluted (0.01% *V/V*) and therefore it could not be visualized in a straightforward manner, though it may be responsible for some lighter shadows on the image.

The chemical composition of graphene, GO and rGO was assessed with X-ray photoelectron spectroscopy (XPS). Figs. 3A and B display two well-defined binding energy peaks for graphene and GO at 285.4 eV assigned to C_{1s} (graphene = 96.8% and GO = 87.3%) and at 530.9 eV due to O_{1s} (graphene = 3.2% and GO = 12.7%, insets in Figs. 3A and B). With deconvolution of the XPS spectra of C_{1s}, one may determine the degree of oxidation and the binding of carbon atoms: aromatic C–C bonds (carbon sp^2, 284.5 eV); C–H (285.6 eV); C–O (ether/alcohol, 286.5 eV), C=O (carbonyl, 287.6 eV), O–C=O (carboxyl, 289.5 eV). There was a large difference in peak intensity between graphene and GO. For graphene the aromatic bond (C–C) peak was large, indicating the expected high degree of order of the hexagonal carbon structure. On the other hand, for GO there was an increase in the peaks related to carbon bonds with oxygenated groups (CO, C=O and O–C=O) and CH, with a consequent decrease in the peak related to aromatic C–C. This confirmed that oxygenated groups were inserted in the carbon structure of graphene.

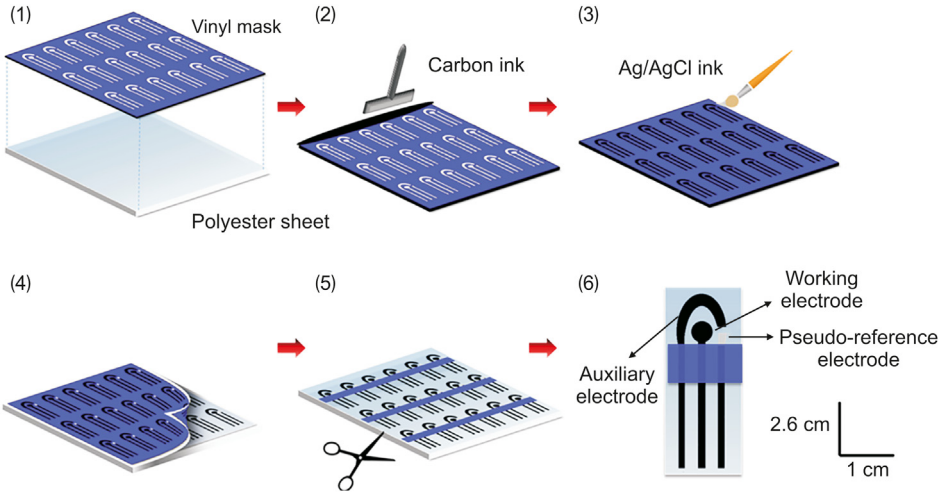

Fig. 1. Schematic representation of the preparation of screen-printed electrode (SPE).

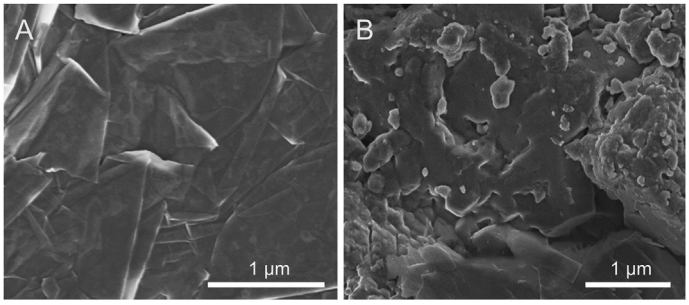

Fig. 2. Morphological characterization by scanning electron microscopy images of (A) reduced graphene oxide (rGO) and (B) C60-rGO.

When GO was reduced using $NaBH_4$, these groups were removed, and their corresponding peaks decreased significantly, as shown in Fig. 3C for rGO.

3.2. Catalytic activity from synergic effect between C60 and rGO

The analytic response of the C60-rGO-NF/SPE sensor was determined using cyclic voltammetry for a concentration of MTZ of 1.0×10^{-4} mol/L. Fig. 4 shows the cathodic peak due to reduction of MTZ on the electrode surface at −0.9 V vs. Ag/AgCl (3.0 mol/L KCl). This peak increased when the SPE electrode was modified with C60 and rGO, with the current for C60-rGO-NF/SPE being 5 times the value for SPE and 2.1 times the value for rGO/SPE. The increased current can be attributed to an increase in the porosity of these nanomaterials which increases the surface area of the electrode. The electrochemical reduction of MTZ involves four electrons according to reaction below [42].

$$R{-}NO_2 + 4e^- + 4H^+ \rightarrow R{-}NHOH + H_2O$$

where

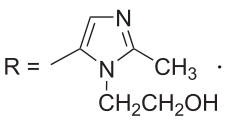

3.3. Effect of potential scan rate and pH

The presence of a cathodic peak and absence of anodic peaks in Fig. 5 indicate an irreversible redox process for MTZ on the C60-rGO-NF/SPE sensor. The cathodic peak shifted to a more negative potential and increased with the scan rate. The insets show that the cathodic peak current decreased linearly with the scan rate, with a correlation coefficient of 0.998. We also tried the $v^{1/2}$ dependence but fitting was poorer, with a correlation coefficient of 0.967. Therefore, the MTX redox reaction was controlled by an adsorption process (rather than a diffusion process).

Fig. S1 shows that the cathodic peak current for MTZ increased with the pH up to pH 7, above which it leveled off. This is why we selected pH 7 for subsequent experiments to determine MTZ with the C60-rGO-NF/SPE sensor. The potential at which the cathodic peak occurred increased with pH, as is typical of an irreversible electrochemical process. The equation for the E_p vs. pH in Fig. S1 is E_p=−0.4−0.062pH, where the slope of −0.062 mV/pH corresponds to an equal number of protons and electrons in the electrochemical reduction of MTZ [51].

3.4. Determination of MTZ using the C60-rGO-NF/SPE sensor

First, a comparison was made between differential pulse voltammetry and square wave voltammetry (SWV). From the analysis of peak current intensity and stability in the electrochemical signal, we inferred that SWV presented the best response. Thus, this technique was chosen for the detection and quantification studies of MTZ. The quantitative determination of MTZ was performed under optimized conditions for the C60-rGO-NF/SPE sensor. Fig. 6 shows a linear increase in the peak current with MTZ concentration in the range between 2.5×10^{-7} and 34×10^{-6} mol/L, with a regression equation I_p (μA) = 0.15 + 0.1C_{MTZ} (μmol/L) (r=0.998). The limit of detection (LOD) was 2.1×10^{-7} mol/L, calculated using the statistical method described by da Silva and Machado [52], LOD = $y_B + 3S_B$, where y_B is the intercept of the calibration plot used as the blank signal and S_B is the standard deviation (obtained directly from the analytical curve). The concentrations for which the sensor works are clinically relevant as they correspond to serum concentrations from patients reported in the literature. For instance, after administering a single dose of 200 mg MTZ, the blood concentration varied from 5.8×10^{-7} mol/L to 2.8×10^{-6} mol/L within 24 h and with a renal excretion of 13%–46% [53]. In subsidiary experiments we verified that the sensor displayed a linear behavior for MTZ concentrations up to 10^{-6} mol/L (not shown). We also tested the accumulation potential (E_{acc}) at potentials 0, −0.2, and −0.4 V with an accumulation time of 30 s, and

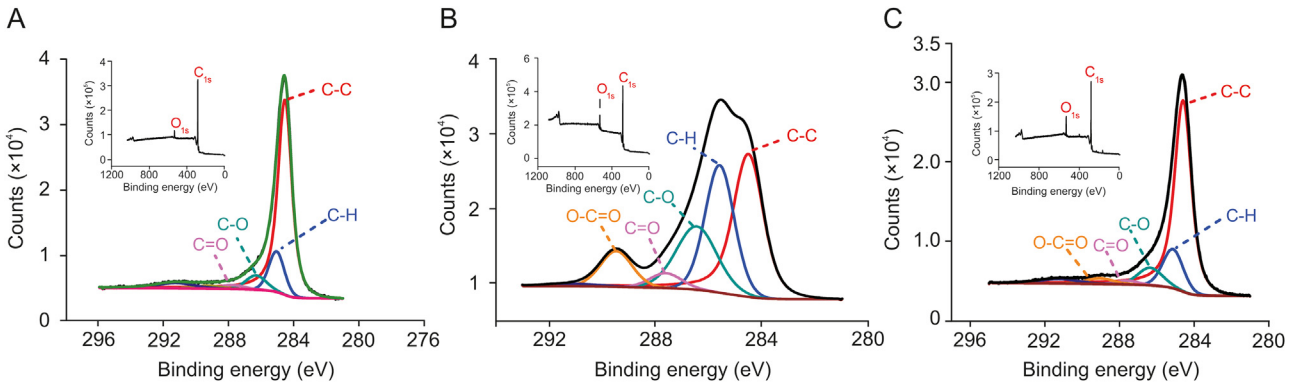

Fig. 3. Evaluation of graphene functionalization by X-ray photoelectron spectroscopy analysis: (A) graphene, (B) GO and (C) rGO, and respective insets.

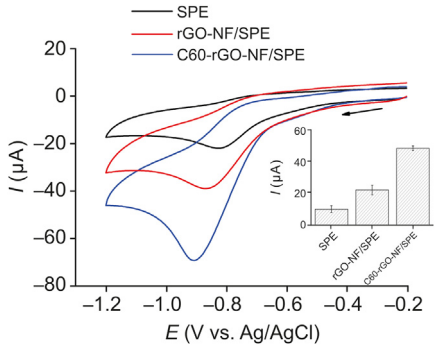

Fig. 4. Cyclic voltammograms of 1.0×10^{-4} mol/L metronidazole (MTZ) in 0.1 mol/L phosphate buffer (pH 7.0) for bare SPE, rGO-NF/SPE and C60-rGO-NF/SPE. Scan rate=25 mV/s. NF: Nafion.

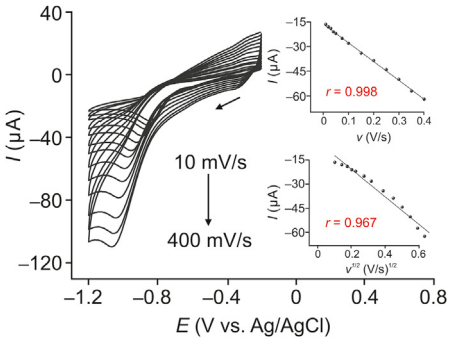

Fig. 5. Effect of different scan rates on cyclic voltammograms at the C60-rGO-NF/SPE sensor in the presence of 5.0×10^{-5} mol/L MTZ in 0.1 mol/L phosphate buffer (pH 7.0).

did not observe an appreciable increase in current. This is favorable for the electrochemical analysis, and E_{acc} was not used for determining MTZ in the SWV experiments.

Table 1 shows that LOD and linear range for the C60-rGO-NF/SPE sensor are competitive with other electrochemical devices to determine MTZ in the literature [36,38–40,42–44,54]. Furthermore, this sensor is highly stable, providing repeatable results with small sample volumes. The whole methodology is also promising because it is amenable to mass production of electrodes at a low cost, which is essential for disposable devices.

3.5. Interference and repeatability studies

The repeatability of the electrochemical signal for MTZ using C60-rGO-NF/SPE sensor was evaluated in 0.1 mol/L phosphate buffer solution containing 5.0×10^{-6} mol/L MTZ in 14 measurements. The relative standard deviation (RSD) of the cathodic peak current was 3.6% (Fig. S2). When different electrodes were employed, RSD was 4.9% (for seven electrodes, i.e., n=7). Hence, the proposed sensor had a good repeatability. The influence of possible interferents in plasma and urine for MTZ determination was found to be negligible, as demonstrated in Fig. 7, when several drugs and substances were added to MTZ. There was no significant change in the MTZ analytical signal, when clindamycine, diclofenac, tetracycline, dopamine, uric acid, dipyrone, ranitidine and caffeine were tested in SWV experiments using a 1:1 concentration ratio (analyte:interference). In addition, no change in analytical signal was observed for a 1:10 concentration ratio (analyte:interference). The MTZ concentration used was 5.0×10^{-7} mol/L, while the interferent concentration was 5.0×10^{-6} mol/L.

3.6. Analytical applications to urine and serum samples

Proof-of-concept experiments were performed to determine MTZ in synthetic serum and urine samples. Table 2 shows the SWV results for the C60-rGO-NF/SPE sensor under the same conditions identified in the optimization process. Recovery of MTZ ranged from 94% to 100% with RSD of 3.3% in triplicate experiments for serum and urine samples. Significantly, the relative error in these results was within 10% of the values obtained with the standard HPLC method (Fig. S3).

4. Conclusion

We have designed an electrochemical sensor that can be employed in therapeutic drug monitoring, for which distinct

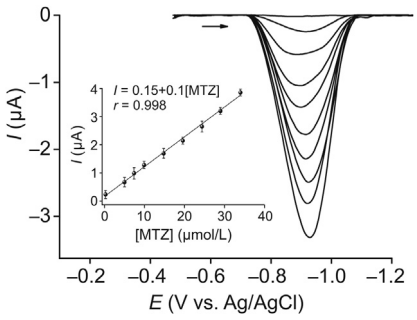

Fig. 6. SWV at C60-rGO-NF/SPE sensor for different concentrations of MTZ in a phosphate buffer (pH=7.0) and analytical curve (inset). Parameters square wave voltammetry (SWV): f=15 Hz, A=75 mV, and ΔE=5 mV.

Table 1
Comparison of analytical results for the C60-rGO-NF/SPE sensor with other methods to determine metronidazole in the literature.

Electrode sensor	Method	Linear range (μmol/L)	LOD (μmol/L)	Refs.
MIP/MWCNT/GCE[a]	CV	1.2–20	0.00029	[36]
3D-HPG/PTH/GCE[b]	CV	0.05–70	0.001	[38]
Ni/Fe-LDH electrode[c]	Amperometry	5.0–1610	58	[39]
Polydopamine/MWCNTs–COOH nanocomposites/GCE[d]	DPV	5–5000	0.25	[40]
LDH/CQDs@CPE[e]	DPV	1.5–300	0.2	[42]
CPE[f]	SWV	1–100	0.99	[43]
CPE-CD[g]	DPV[i]	0.5–103	0.28	[44]
Carbon fibre microdisk electrode	SWV[h]	1.0–2.2	0.5	[54]
C60-rGO-NF/SPE	SWV	0.25–34.0	0.21	**This work**

[a] Molecularly imprinted polymer (MIP) and multi-walled carbon nanotubes (MWCNT) modified glassy carbon electrode (GCE).
[b] Graphene-like carbon architecture and polythionine modified GCE.
[c] Ni/Fe-layered double hydroxides (Ni/Fe-LDH) on the GCE.
[d] Polydopamine and carboxylic MWCNT modified GCE.
[e] LDH and carbon quantum dots (CQD)@carbon paste electrode.
[f] Carbon paste electrode.
[g] Electropolymerization of a-cyclodextrin on carbon paste electrode.
[h] Square wave voltammetry.
[i] Differential pulse voltammetry.

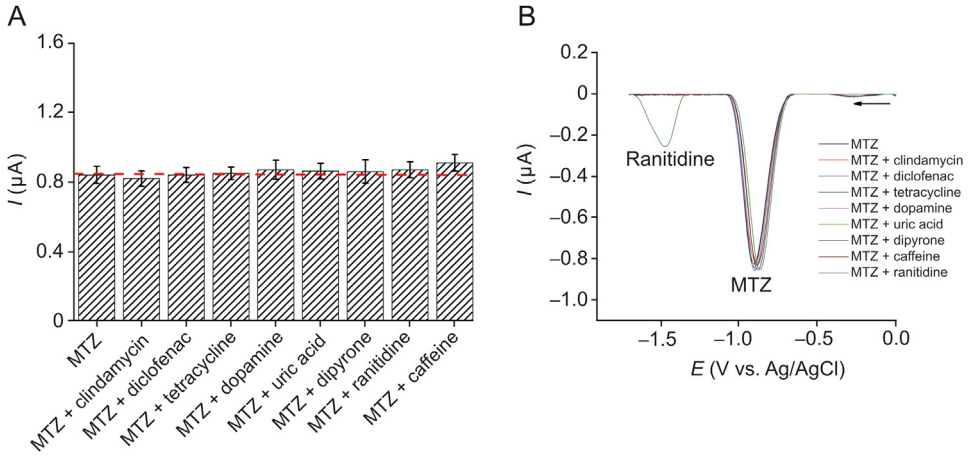

Fig. 7. (A) Study of interference with different drugs and (B) SWV graph.

Table 2
Results from the analysis of synthetic urine and serum samples using C60-rGO-NF/SPE sensor under optimized conditions. The last column shows the relative error compared with the standard HPLC method.

Matrices	Added (mol/L)	$Found_{Proposed\ method}$[a] (mol/L)	$Found_{Comparative\ method}$[a] (mol/L)	Recovery[b] (sensor, %)	Relative error[c]
Urine	1.0×10^{-6}	$(9.6 \pm 0.1) \times 10^{-7}$	$(9.5 \pm 0.1) \times 10^{-7}$	96	−3.2
	1.0×10^{-5}	$(9.4 \pm 0.2) \times 10^{-6}$	$(9.4 \pm 0.1) \times 10^{-6}$	94	0
Serum	1.0×10^{-6}	$(1.0 \pm 0.2) \times 10^{-6}$	$(1.1 \pm 0.1) \times 10^{-6}$	100	−9.1
	1.0×10^{-5}	$(9.5 \pm 0.3) \times 10^{-6}$	$(9.9 \pm 0.1) \times 10^{-6}$	95	4.0

[a] Average of 3 concentrations.
[b] Recovery percentage = $(Found_{Proposed\ method}/added) \times 100$.
[c] Relative error = $[(Found_{Proposed\ method} - Found_{Comparative\ method})/Found_{Comparative\ method}] \times 100$.

carbon nanomaterials were combined. The suitability of the methodology was demonstrated with the antibiotic MTZ, which could be determined with an LOD of 2.1×10^{-7} mol/L using the C60-rGO-NF/SPE sensor. Furthermore, this sensor could be applied to determine MTZ in urine and serum samples, with recoveries similar to those of the standard HPLC-UV technique. The method exhibits high stability, repeatability and reproducibility. The high performance of the sensor may be attributed to the synergy in electrocatalytic activity of C60 and rGO, as indicated by the results with cyclic voltammetry and SWV. The fast response and low cost of the electrochemical sensors require a small expenditure of materials and reagents. The materials, concepts, and methodology are generic and may be extended to other antibiotics and drugs, and this is promising for drug monitoring to fight bacteria resistance.

Declaration of competing interest

The authors declare that there are no conflicts of interest.

Acknowledgments

The authors gratefully acknowledge the financial support

granted by CNPq, INEO, CAPES and FAPESP (Grant Nos.: 2018/22214-6, 2017/24053-7 and 2016/0991-5).

Appendix A. Supplementary data

Supplementary data to this article can be found online at https://doi.org/10.1016/j.jpha.2021.03.004.

References

[1] C.L. Ventola, The antibiotic resistance crisis Part 1 : causes and threats, Pharmacol. Ther. 40 (2015) 277–283.
[2] A. Fournier, P. Eggimann, O. Pantet, et al., Impact of real-time therapeutic drug monitoring on the prescription of antibiotics in burn patients requiring admission to the intensive care unit, Clin. Therapeut. 62 (2018) 1–17.
[3] D. Horn, C. Klaas, M. Fobker, et al., Therapeutic Drug Monitoring of Antibiotics in Critically Ill Patients, in: Handbook of Analytical Separations, Vol. 7, Elsevier, Amsterdam, 2020, pp. 169–183.
[4] J.A. Roberts, R. Norris, D.L. Paterson, et al., Therapeutic drug monitoring of antimicrobials, Br. J. Clin. Pharmacol. 73 (2011) 27–36.
[5] C. Mabilat, M.F. Gros, D. Nicolau, et al., Diagnostic and medical needs for therapeutic drug monitoring of antibiotics, Eur. J. Clin. Microbiol. Infect. Dis. 39 (2020) 791–797.
[6] J. Kang, M.H. Lee, Overview of therapeutic drug monitoring, Korean J. Intern. Med. 24 (2019) 1–10.
[7] R. Companyó, M. Granados, J. Guiteras, et al., Antibiotics in food : legislation and validation of analytical methodologies, Anal. Bioanal. Chem. 395 (2009) 877–891.
[8] I.A. Darwish, Immunoassay Methods and their applications in pharmaceutical analysis : basic methodology and recent advances, Int. J. Biomed. Sci. 2 (2006) 217–235.
[9] V. Pérez-Fernández, E. Dominguez-Vega, A.L. Crego, et al., Recent advances in the analysis of antibiotics by CE and CEC, Electrophoresis 33 (2012) 127–146.
[10] A. Pollap, J. Kochana, Electrochemical immunosensors for antibiotic detection, Biosensors 9 (2019) 4325–4329.
[11] E. Zacco, J. Adrian, R. Galve, et al., Electrochemical magneto immunosensing of antibiotic residues in milk, Biosens. Bioelectron. 22 (2007) 2184–2191.
[12] F.-D. Munteanu, A.M. Titoiu, J.-L. Marty, et al., Detection of antibiotics and evaluation of antibacterial activity with screen-printed electrodes, Sensors 18 (2018) 901–925.
[13] V.A. Online, M. Jacobs, V.J. Nagaraj, et al., Analytical Methods an electrochemical sensor for the detection of antibiotic, Anal. Methods. 5 (2013) 4325–4329.
[14] H.S. Stevenson, S.S. Shetty, N.J. Thomas, et al., Ultrasensitive and rapid-response sensor for the electrochemical detection of antibiotic residues within meat samples, ACS Omega 4 (2019) 6324–6330.
[15] Z. Li, C. Liu, V. Sarpong, et al., Multisegment nanowire/nanoparticle hybrid arrays as electrochemical biosensors for simultaneous detection of antibiotics, Biosens. Bioelectron. 126 (2019) 632–639.
[16] M. Elfiky, N. Salahuddin, A. Hassanein, et al., Detection of antibiotic Ofloxacin drug in urine using electrochemical sensor based on synergistic effect of different morphological carbon materials, Microchem. J. 146 (2019) 170–177.
[17] X. Liu, D. Huang, C. Lai, et al., Recent advances in sensors for tetracycline antibiotics and their applications, Trac-trend. Anal. Chem. 109 (2018) 260–274.
[18] V. Biju, Chemical modifications and bioconjugate reactions of nanomaterials for sensing, imaging, drug delivery and therapy, Chem. Soc. Rev. 43 (2014) 744–764.
[19] A. Zhang, C.M. Lieber, Nano-bioelectronics, Chem. Eng. Sci. 116 (2016) 215–257.
[20] J. Siegrist, R. Gorkin, M. Bastien, et al., Validation of a centrifugal microfluidic sample lysis and homogenization platform for nucleic acidextraction with clinical samples, Lab Chip 10 (2010) 363–371.
[21] S.J. Rowley-Neale, E.P. Randviir, A.S. Abo, et al., An overview of recent applications of reduced graphene oxide as a basis of electroanalytical sensing platforms, Appl. Mater. Today. 10 (2018) 218–226.
[22] S. Kurbanoglu, S.A. Ozkan, Electrochemical carbon based nanosensors : a promising tool in pharmaceutical and biomedical analysis, J. Pharm. Biomed. Anal. 147 (2018) 439–457.
[23] P. Yáñez-Sedeño, S. Campuzano, J.M. Pingarrón, Fullerenes in electrochemical catalytic and affinity biosensing: a review, C-J. Carbon Res. 3 (2017), 21.
[24] S. Afreen, K. Muthoosamy, S. Manickam, et al., Functionalized fullerene (C 60) as a potential nanomediator in the fabrication of highly sensitive biosensors, Biosens. Bioelectron. 63 (2015) 354–364.
[25] S. Pilehvar, K. De Wael, Recent advances in electrochemical biosensors based on fullerene-C60 nano-structured platforms, Biosensors (Basel). 5 (2015) 712–735.
[26] N.P. Shetti, S.J. Malode, S.T. Nandibewoor, Electrochemical behavior of an antiviral drug acyclovir at fullerene-C60-modified glassy carbon electrode, Bioelectrochemistry 88 (2012) 76–83.
[27] R.N. Goyal, V.K. Gupta, N. Bachheti, Fullerene-C60-modified electrode as a sensitive voltammetric sensor for detection of nandrolone—an anabolic steroid used in doping, Anal. Chim. Acta 597 (2007) 82–89.
[28] J. Carlos, R. Ledezma, Therapeutic uses of metronidazole and its side effects : an update, Eur. Rev. Med. Pharmacol. Sci. 23 (2019) 397–401.
[29] C.M. Rao, A. Ghosh, C. Raghothama, et al., Does metronidazole reduce lipid peroxidation in burn injuries to promote healing? Burns 28 (2002) 427–429.
[30] D. Bracco, P. Eggimann, Prophylaxis with systemic antibiotics in patients with severe burns, Br. Med. J. 340 (2010) 10–12.
[31] L. Azimi, R. Alaghehbandan, M. Asadian, et al., Multi-drug resistant Pseudomonas aeruginosa and Klebsiella pneumoniae circulation in a burn hospital, Tehran, Iran, GMS Hyg. Infect. Control 14 (2019) 1–5.
[32] Y. Li, Y. Liu, Y. Yang, et al., Novel electrochemical sensing platform based on a molecularly imprinted polymer decorated 3D nanoporous nickel skeleton for ultrasensitive and selective determination of metronidazole, ACS Appl. Mater. Interfaces 7 (2015) 15474–15480.
[33] H. Song, L. Zhang, F. Yu, et al., Molecularly imprinted polymer functionalized nanoporous Au-Ag alloy microrod : novel supportless electrochemical platform for ultrasensitive and selective sensing of metronidazole, Electrochim. Acta 208 (2016) 10–16.
[34] Y. Gu, X. Yan, C. Li, et al., Biomimetic sensor based on molecularly imprinted polymer with nitroreductase-like activity for metronidazole detection, Biosens. Bioelectron. 77 (2016) 393–399.
[35] A.A. Ensafi, P. Nasr-Esfahani, B. Rezaei, Metronidazole determination with an extremely sensitive and selective electrochemical sensor based on graphene nanoplatelets and molecularly imprinted polymers on graphene quantum dots, Sensor. Actuator. B Chem. 270 (2018) 192–199.
[36] Y. Liu, J. Liu, H. Tang, et al., Fabrication of highly sensitive and selective electrochemical sensor by using optimized molecularly imprinted polymers on multi-walled carbon nanotubes for metronidazole measurement, Sensor. Actuator. B Chem. 206 (2015) 647–652.
[37] Y. Gu, W. Liu, R. Chen, et al., β-cyclodextrin-functionalized gold nanoparticles/poly (L-cysteine) modified glassy carbon electrode for sensitive determination of metronidazole, Electroanalysis 25 (2013) 1209–1216.
[38] M. Yang, M. Guo, Y. Yu, et al., Sensitive voltammetric detection of metronidazole based on three-dimensional graphene-like carbon architecture/polythionine modified glassy carbon electrode, J. Electrochem. Soc. 165 (2018) 530–535.
[39] K. Nejati, K. Asadpour-Zeynali, Electrochemical synthesis of nickel–iron layered double hydroxide: application as a novel modified electrode in electrocatalytic reduction of metronidazole, Mater. Sci. Eng. C. Mat. Bio. Appl. 35 (2014) 179–184.
[40] S. Tursynbolat, Y. Bakytkarim, J. Huang, et al., Ultrasensitive electrochemical determination of metronidazole based on polydopamine/carboxylic multi-walled carbon nanotubes nanocomposites modified GCE, J. Pharm. Anal. 8 (2018) 124–130.
[41] W. Liu, J. Zhang, C. Li, et al., A novel composite film derived from cysteic acid and PDDA-functionalized graphene: enhanced sensing material for electrochemical determination of metronidazole, Talanta 104 (2013) 204–211.
[42] S. Alizadeh, M. Hasanzadeh, A novel electrochemical sensor based on LDH/CQD @ Carbon paste electrode for voltammetric determination of metronidazole in real Samples, Int. J. Sci. Eng. Res. 9 (2018) 466–475.
[43] Y. Nikodimos, M. Amare, Electrochemical determination of metronidazole in tablet samples using carbon paste electrode, J. Anal. Methods Chem. 2016 (2016), 3612943.
[44] A. Hernández-Jiménez, G. Roa-Morales, H. Reyes-Pérez, et al., Voltammetric determination of metronidazole using a sensor based on electropolymerization of α-cyclodextrin over a carbon paste electrode, Electroanalysis 28 (2016) 704–710.
[45] B.M. Tashtoush, E.L. Jacobson, M.K. Jacobson, Validation of a simple and rapid hplc method for determination of metronidazole in Dermatological, Drug Dev. Ind. Pharm. 34 (2008) 840–844.
[46] A.S. Afonso, C.V. Uliana, D.H. Martucci, et al., Simple and rapid fabrication of disposable carbon-based electrochemical cells using an electronic craft cutter for sensor and biosensor applications, Talanta 146 (2016) 381–387.
[47] R.A.G. De Oliveira, E.M. Materon, M.E. Melendez, et al., Disposable microfluidic immunoarray device for sensitive breast cancer Biomarker Detection, ACS Appl. Mater. Interfaces 9 (2017) 27433–27440.
[48] R.N. Goyal, S.P. Singh, Voltammetric determination of paracetamol at C60 -modified glassy carbon electrode, Electrochim. Acta 51 (2006) 3008–3012.
[49] N. Laube, B. Mohr, A. Hesse, Laser-probe-based investigation of the evolution of particle size distributions of calcium oxalate particles formed in artificial urines, J. Cryst. Growth 233 (2001) 367–374.
[50] H. Parham, B. Zargar, Determination of isosorbide dinitrate in arterial plasma , synthetic serum and pharmaceutical formulations by linear sweep voltammetry on a gold electrode, Talanta 55 (2001) 255–262.
[51] A.J. Bard, L.R. Faulkner, Electrochemical Methods, Fundamentals and

Applications, John Wiley & Sons, Inc, New York, 1980, pp. 98.
[52] O.B. da Silva, S.A.S. Machado, Evaluation of the detection and quantification limits in electroanalysis using two popular methods: application in the case study of paraquat determination, Anal. Methods 4 (2012) 2348–2354.
[53] P. Kane, J.A. Mcfadzean, S. Squires, et al., Absorption and excretion of metronidazole.Part I. Serum concentration and unrinary excretion after oral administration, Br. J. Vener. Dis. 37 (1961) 273–275.
[54] P.N. Bartlett, E. Ghoneim, G. El-Hefnawy, et al., Voltammetry and determination of metronidazole at a carbon fiber microdisk electrode, Talanta 66 (2005) 869–874.